

Development 138, 4813 (2011) doi:10.1242/dev.075044
© 2011. Published by The Company of Biologists Ltd

Motoneurons are essential for vascular pathfinding

Amy H. Lim, Arminda Suli, Karina Yaniv, Brant Weinstein, Dean Y. Li and Chi-Bin Chien

There were errors published in *Development* **138**, 3847-3857.

Three morpholinos were incorrectly described in the materials and methods section Morpholino (MO) oligonucleotide injections. For the *olig2* and *robo4* MOs, the incorrect sequence was shown; in addition, the *olig2* MO was described as splice blocking instead of translation blocking. The *mtp* MO was incorrectly described as unpublished. Corrected information for these three MOs appears below.

The authors apologise to readers for these mistakes.

olig2 translation-blocking MO: 5'-CGTTCAGTGCCTCTCAGCTTCTCG-3'

robo4 MO: 5'-TTTTTTAGCGTACCTATGAGCAGTT-3'

mtp MO: 5'-CGGCAACCGGCATCATGTTTGGG-3' (Schlegel and Stainier, 2006)

Reference
Schlegel, A. and Stainier, D. Y. (2006). Microsomal triglyceride transfer protein is required for yolk lipid utilization and absorption of dietary lipids in zebrafish larvae. *Biochemistry* **45**, 15179-15187

Motoneurons are essential for vascular pathfinding

Amy H. Lim^{1,2,*}, Arminda Suli^{2,*}, Karina Yaniv³, Brant Weinstein⁴, Dean Y. Li^{1,5,6,†} and Chi-Bin Chien²

SUMMARY

The neural and vascular systems share common guidance cues that have direct and independent signaling effects on nerves and endothelial cells. Here, we show that zebrafish Netrin 1a directs Dcc-mediated axon guidance of motoneurons and that this neural guidance function is essential for lymphangiogenesis. Specifically, Netrin 1a secreted by the muscle pioneers at the horizontal myoseptum (HMS) is required for the sprouting of *dcc*-expressing rostral primary motoneuron (RoP) axons and neighboring axons along the HMS, adjacent to the future trajectory of the parachordal chain (PAC). These axons are required for the formation of the PAC and, subsequently, the thoracic duct. The failure to form the PAC in *netrin 1a* or *dcc* morphants is phenocopied by laser ablation of motoneurons and is rescued both by cellular transplants and overexpression of *dcc* mRNA. These results provide a definitive example of the requirement of axons in endothelial guidance leading to the parallel patterning of nerves and vessels in vivo.

KEY WORDS: Netrin, DCC, Lymphatic, Parachordal chain, Motoneuron, Axon guidance, Vascular guidance, Angiogenesis, Zebrafish

INTRODUCTION

There is a striking congruence among the anatomies of nerves, blood vessels and lymphatics. Not surprisingly, the prototypic guidance cues, initially discovered for their roles in axon pathfinding (Dickson, 2002), also guide blood vessels and lymphatics (Adams and Eichmann, 2010; Carmeliet and Tessier-Lavigne, 2005; Larrivee et al., 2009; Melani and Weinstein, 2009; Suchting et al., 2006; Weinstein, 2005). One such family, the Netrins, directly guide both axon outgrowth and vascular sprouting through various receptors. Depending on the receptors expressed, Netrins may be repulsive or attractive (Bouvier et al., 2008; Cirulli and Yebra, 2007; Hong et al., 1999; Larrivee et al., 2007; Lejmi et al., 2008; Lu et al., 2004; Navankasattusas et al., 2008; Park et al., 2004; Rajasekharan and Kennedy, 2009; Wilson et al., 2006). Netrins also act as a survival cue for dependence receptors in shaping the neural and vascular systems during development (Castets et al., 2009; Furne et al., 2008; Tang et al., 2008).

The close alignment of nerves and vessels throughout the body plan could be achieved in one of two ways: either by shared patterning mechanisms or by axons acting to guide vessels (or vice versa). For example, in the developing quail forelimb, nerves and

vessels both respond with repulsion to Sema3A/Nrp1 signaling (Bates et al., 2003). By contrast, a subset of axonal projections from the superior cervical ganglion specifically follows Endothelin 3 secreted by the external carotid artery (Makita et al., 2008). Conversely, motoneurons, sensory neurons and/or Schwann cells secrete Vegf that is required for arterial differentiation in the skin (Mukoyama et al., 2005). Therefore, when investigating the effects of axon guidance cues on blood vessels or lymphatic endothelium, it is essential to distinguish a direct effect on endothelial cells from the potential influence on axonal projections, which may subsequently affect the endothelial cells.

The parachordal chain (PAC), a string of endothelial cells located at the horizontal myoseptum (HMS), forms at 2 days post-fertilization (dpf) in zebrafish. Since the PAC bears no evidence of a lumen (Hogan et al., 2009a), we prefer this nomenclature to the previous term ‘parachordal vessel’. The PAC cells eventually migrate ventrally along the trunk vasculature to the space between the dorsal aorta (DA) and the posterior cardinal vein (PCV) to form the main vessel of the lymphatic system: the thoracic duct (TD) (Bussmann et al., 2010; Yaniv et al., 2006). Prior to the formation of the PAC along the HMS, however, motoneurons extend axons along a path parallel to its future trajectory (Beattie, 2000; Eisen et al., 1986; Pike and Eisen, 1990), offering an opportunity to dissect the contribution of neurons and endothelial cells to zebrafish lymphatic patterning and development.

We previously showed that knockdown of *netrin 1a*, a zebrafish ortholog of mammalian netrin 1, disrupts PAC development (Wilson et al., 2006). In the current study, we definitively identify the muscle pioneers (MPs) as the critical source of Netrin 1a for PAC formation. We show that *netrin 1a* and *dcc* are required for three precise events: axonal extension of RoP and secondary motoneurons (SMNs) along the HMS; the turn made by secondary vascular sprouts to follow the HMS; and the formation of the PAC. Furthermore, genetic removal or laser ablation of the motoneurons also prevents secondary sprout turning and PAC formation. These results show that lymphangiogenesis is dependent on choreographed interactions between MPs, axons and endothelial cells. In particular, growth of the RoP axon and associated axons determines the guidance of the PAC lymphendothelial cells.

¹Molecular Medicine Program, 15 N 2030 East, Room 4140, University of Utah, Salt Lake City, UT 84112, USA. ²Department of Neurobiology and Anatomy, 20 North 1900 East, Room 401 MREB, University of Utah, Salt Lake City, UT 84132, USA.

³Department of Biological Regulation, Weizmann Institute of Science, Rehovot, 76100, Israel. ⁴Laboratory of Molecular Genetics, National Institute of Child Health and Human Development, National Institutes of Health, Building 6B, Room 309, 6 Center Drive, Bethesda, MD 20892, USA. ⁵Division of Cardiology, Department of Medicine, 30 N 1900 East, Room 4A100 SOM, University of Utah, Salt Lake City, UT 84132, USA. ⁶Department of Oncological Sciences, 2000 Circle of Hope, University of Utah, Salt Lake City, UT 84112, USA.

*These authors contributed equally to this work

†Author for correspondence (dean.li@u2m2.utah.edu)

This is an Open Access article distributed under the terms of the Creative Commons Attribution Non-Commercial Share Alike License (<http://creativecommons.org/licenses/by-nc-sa/3.0>), which permits unrestricted non-commercial use, distribution and reproduction in any medium provided that the original work is properly cited and all further distributions of the work or adaptation are subject to the same Creative Commons License terms.

MATERIALS AND METHODS

Fish stocks and embryo raising

Zebrafish adults were maintained and bred according to standard procedures. Tg(*fli1a:egfp*)^{y1/+} fish were a gift from Joe Yost (University of Utah). *plcg*^{y10/+}; Tg(*fli1a:egfp*)^{y1/+} and Tg(*fli1a-ep:DsRedEx*)^{uml3} fish were a gift from Nathan Lawson (University of Massachusetts). *isl1*^{sa0029/+}; Tg(*fli1a:egfp*)^{y1/+} were from the Sanger Institute Zebrafish Mutation Resource. Tg(*hb9:GFP*) fish (official name *mx1:gfp*^{ml2}) and Tg(*hb9:KikGR*)^{p151}; *fli1a1:egfp* fish were gifts from Michael Granato (Flanagan-Steet et al., 2005). All experiments were carried out subject to NIH guidelines and approved by the University of Utah Institutional Animal Care and Use Committee.

Morpholino oligonucleotide (MO) injections

We injected the following MOs from Gene Tools (Philomath, OR, USA): standard control MO (Control), 5'-CCTCTACCTCAGTTACAATTATA-3'; 6-10 ng *netrin 1a* splice-blocking MO (*netrin1aSBMO*), 5'-ATGATGGACTTACCGACACATTCGT-3' (Wilson et al., 2006); 8.6 ng *dcc* translation-blocking MO (*dccTBMO*), 5'-GAATATCTC-CAGTGACGCAGCCCAT-3' (Suli et al., 2006) (+1 to +25 bp, reverse strand start codon underlined); 10.2 ng *olig2* splice-blocking MO (*olig2SBMO*), 5'-CGTTCAGTGCCTCTCAGCTTG-3' (Park et al., 2002); 15.3 ng *plcg1* MO (*plcg1SBMO*), 5'-ATTAGCATAGGGAAC-TTACTTTCG-3' (Lawson et al., 2003); 6.0 ng *isl1E2* splice-blocking MO, 5'-TTAATCTGCGTTACCTGATGTAGTC-3' and 6.0 ng *isl1E3* MO, 5'-GAATGCAATGCCTACCTGCCATTTG-3' were injected sequentially (Hutchinson and Eisen, 2006). It should be noted that MOs targeted against non-Netrin-related transcripts were injected in other experiments and a PAC and/or axon phenotype at the HMS was not observed: *roundabout 4* (*robo4*), 5'-TTTTTAGCGTACCTATGAGCAGTT-3' (Bedell et al., 2005); *cardiac troponin T2* (*tnt2*), 5'-CATGTTTCTCTGATCTGACACGCA-3' (Sehnert et al., 2002); *hadp1*, 5'-GATCAACTCTTACC-TGCTTGAAAG-3' (Wythe et al., 2011); and *microsomal triglyceride transfer protein* (*mtp*) (unpublished).

dcc mRNA injection

Full-length *Dcc* coding sequence with seven of the first 27 bp mutated (5'-ATGGGATGtGTaCaGGcGAcATcCGC-3') was cloned into a Gateway middle clone (Invitrogen) and combined with p5E-CMV-SP6 and p3E-pA (Kwan et al., 2007) in pDestTol2pA2 and used to synthesize RNA. One-cell stage embryos were first injected with 225 pg *dcc* mRNA, using 0.5% Phenol Red as a marker dye. A subset was then re-injected with 8.6 ng *dccTBMO*.

In situ hybridization (ISH) and immunostaining

ISH for *netrin 1a* and *dcc* was performed as described (Suli et al., 2006). For immunostaining, the following antibodies were used: rabbit anti-GFP primary (1:400; Molecular Probes, Carlsbad, CA, USA) with Alexa 488 anti-rabbit secondary (1:100; Molecular Probes); mouse 4D9 anti-engrailed primary (1:4; Developmental Studies Hybridoma Bank, University of Iowa) with HRP anti-mouse secondary (1:100; Molecular Probes) followed by Alexa 568 tyramide reaction (Molecular Probes); mouse *znp-1* (anti-synaptotagmin 2) (1:200; Developmental Studies Hybridoma Bank, University of Iowa).

Sectioning

Following ISH, embryos were dehydrated in methanol, treated with 1:1 Immuno-Bed:methanol for 30 minutes at 4°C and incubated with undiluted infiltrate overnight at 4°C. The embryos were then embedded with a 20:1 mixture of Immuno-Bed:Immuno-Bed Solution B (Electron Microscopy Sciences) and sectioned at 12 μm in a transverse plane for *netrin 1a* or a longitudinal plane for *dcc*.

Cyclopamine treatment

Thirty embryos per well in a 24-well dish were incubated with 1 ml/well 50 μM cyclopamine in 1% DMSO, or 1% DMSO only as a control, from 50% epiboly to 16 hpf at 23°C, then washed several times with E3 embryo medium (5 mM NaCl, 0.17 mM KCl, 0.33 mM CaCl₂, 0.33 mM MgSO₄).

Cell transplants

One-cell stage *fli1a:egfp*^{y1} embryos were injected with either Rhodamine Dextran (RhDx, 0.5% in water) or 6 ng *netrin1aSBMO*. To target MPs, 5-10 cells were transplanted from 4 hpf RhDx-injected donors into the margin of 3 hpf *netrin 1a* morphant hosts (Halpern et al., 1995). The region between somites 5-15 was scored for PAC defects. The percentage of hemisegments with complete, partial or absent PACs was calculated separately for hemisegments receiving transplanted MPs and those without transplanted MPs, and treated as a paired dataset.

Imaging

z-stack images were acquired (Olympus FV1000 or FV300 confocal microscope) and ImageJ software (Wayne Rasband, NIH) was used to create maximum intensity z-projections; these span only one side of the embryo unless otherwise stated. FluoRender (Wan et al., 2009) was used for volume rendering. For PAC analysis in all experiments except cell transplants and motoneuron ablation, 3-5 hemisegments from somites 7-11 were scored.

Time-lapse imaging

z-stack images (2.5 μm step, ~80 slices) were acquired (Olympus FV1000 confocal microscope). Embryos were imaged every 12-15 minutes for 16.5-19 hours, starting at 29-33 hpf. Room temperature was 27±2°C. Time-lapse movies were generated using maximum intensity projections in ImageJ.

Laser ablation

Using *hb9:KikGR* labeling of motoneuron cell bodies and their stereotypical location relative to the somitic boundary to target the laser, motoneuron cell bodies of *hb9:KikGR; fli1a:egfp*^{y1} embryos at 18-24 hpf were ablated. A 405 nm laser (Olympus FV1000 or FV300 confocal microscope) was used at 100% intensity at 40 μseconds/pixel for 3000 pulses. The embryos were exposed to UV light from a stereomicroscope for ~5-10 seconds to convert the KikGR protein from green to red at 55 hpf and then imaged.

RESULTS

netrin 1a is required for thoracic duct formation

We previously showed that *netrin 1a* is essential for PAC formation (e.g. Wilson et al., 2006). As the PAC has been shown to be the source of lymphatic endothelial cells (LECs) that populate the TD (Geudens et al., 2010; Yaniv et al., 2006), we next investigated whether *netrin 1a* depletion would affect TD development. Embryos injected with *netrin 1a* splice-blocking MO (*netrin1aSBMO*) were assayed for presence of the TD. Whereas embryos injected with a control MO had a complete or partial TD in 77% of their hemisegments (*n*=200 hemisegments, 16 larvae), *netrin 1a* morphants had a complete or partial TD in only 25% of their hemisegments (*n*=292 hemisegments, 24 larvae) (see Fig. S1A-C in the supplementary material). Thus, *netrin 1a* depletion indeed leads to defects in lymphatic development.

netrin 1a is required for attraction of secondary sprouts at the HMS

The absence of the PAC in *netrin 1a*-depleted embryos could result from impaired angiogenesis from the PCV, from defects in the dorsal extension of secondary intersegmental vessel (ISV) sprouts as they grow from the PCV to the HMS, or from defects in turning upon reaching the HMS (Fig. 1A-C'). To determine which of these three steps is affected in the absence of *netrin 1a* we used *plcg*^{y10} mutant embryos because in wild-type (WT) embryos the secondary sprouts track very closely with the ventral portion of the primary ISVs and are difficult to distinguish. *plcg*^{y10} mutants lack primary ISVs but have a normal PCV, secondary sprouts and PAC (Lawson et al., 2003). We injected *plcg*^{y10}; *fli1a:egfp*^{y1} mutants with

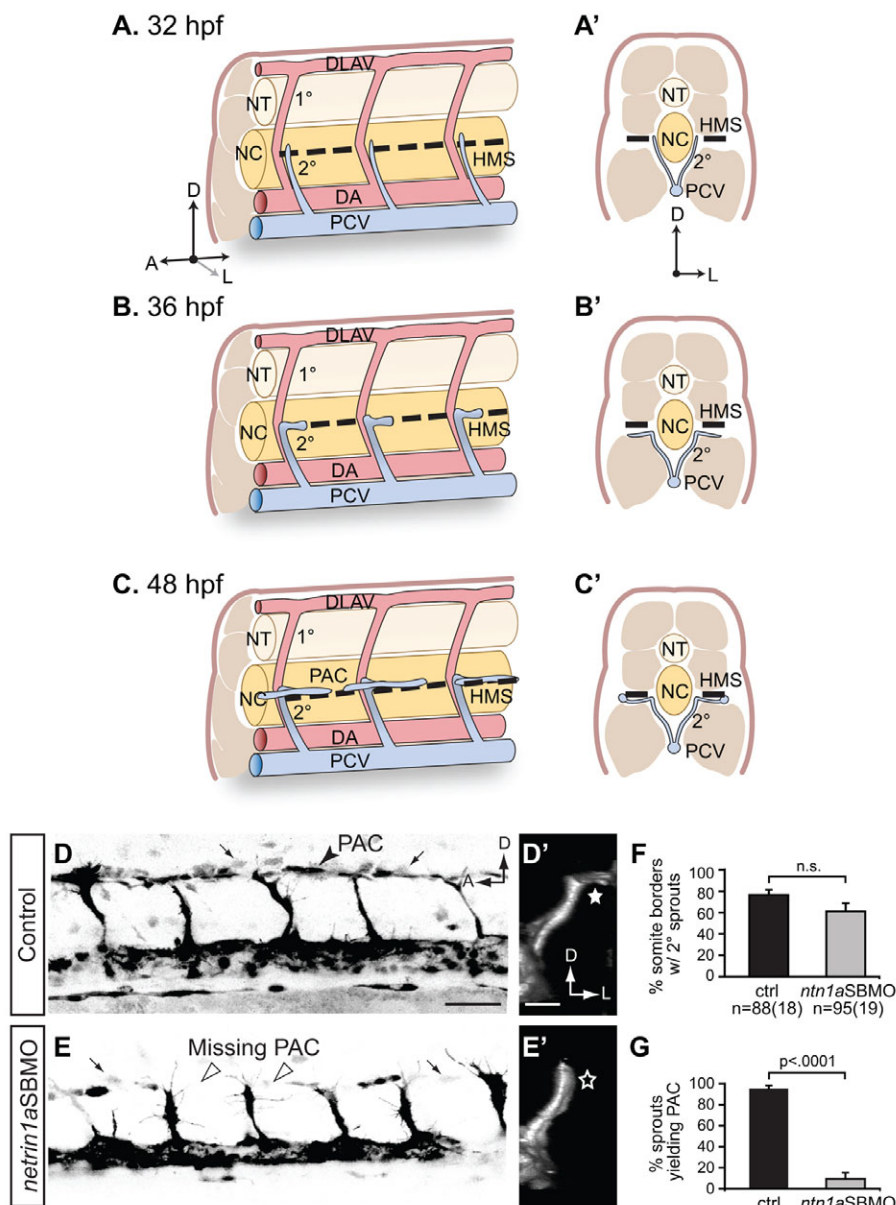


Fig. 1. *netrin 1a* is required for turning of secondary sprouts at the horizontal myoseptum. (A-C') Lateral (A-C) and corresponding transverse views (A'-C') of parachordal chain (PAC) formation, showing dorsal aorta (DA, red), posterior cardinal vein (PCV, blue), horizontal myoseptum (HMS, dashed line), primary intersomitic vessels (1°, red) and secondary sprouts (2°, blue). DA and primary sprouts omitted for clarity. (A,A') Secondary sprouts emerge from the PCV at ~32 hpf and grow dorsally to the HMS. (B,B') Dorsal growth stops at the HMS and sprouts turn and grow laterally. (C') Lateral growth stops at the lateral-most aspect of the muscle, and the sprout then turns anteriorly and posteriorly to form the PAC. (D-E') Removing *netrin 1a* function in 48 hpf *plcg1^{y10}; fli1a:egfp^{y1}* zebrafish embryos. (D,E) Lateral views, reversed contrast. (D',E') Transverse view volume renderings of single hemisegments from D,E. (D,D') In uninjected controls, secondary sprouts grow from the PCV and turn at the HMS (star, D') to form the PAC (arrowhead, D). The *fli1a:egfp^{y1}* transgene also labels some dimly fluorescent non-endothelial cells near the HMS (small arrows, D,E). (E,E') In *netrin 1a* morphants, secondary sprouts usually fail to turn laterally (star, E') and form the PAC (arrowheads, E). (F,G) Secondary sprouts were quantified in five hemisegments per embryo in uninjected controls and *netrin 1a* morphants. (F) The fraction of intersomitic boundaries bearing secondary sprouts is not significantly changed in morphants. Uninjected controls, 75 ± 5%; *netrin 1a* morphants, 61 ± 8%. (G) Fewer secondary sprouts turn to form the PAC in morphants. Uninjected controls, 95 ± 3%; *netrin 1a* morphants, 9 ± 5%. All values are mean ± s.e.m.; error bars show s.e.m.; *P*-value determined by Mann-Whitney U test; n.s., not significant; *n*, number of hemisegments (number of embryos). A, anterior; D, dorsal; L, lateral; DLAV, dorsal longitudinal anastomotic vessel; NT, neural tube; NC, notochord; 1°, primary sprouts; 2°, secondary sprouts. Scale bars: 50 μm.

*netrin1a*SBMO and examined secondary sprout formation (Fig. 1D-F). Secondary sprout formation did not differ from that of uninjected controls (75% of hemisegments with secondary sprout; *n*=88 hemisegments, 18 embryos) and *netrin 1a* morphants (61% of hemisegments with secondary sprout; *n*=95 hemisegments, 19 embryos). In uninjected controls, secondary sprouts extended dorsally to the HMS (Fig. 1D), turned laterally (Fig. 1D') and then extended anteroposteriorly to form the PAC (Fig. 1D). In morphants, secondary sprouts extended normally to the HMS (Fig. 1E) but then failed to turn laterally or anteroposteriorly (Fig. 1E'). Whereas in controls 95% of secondary sprouts turned at the HMS to form a PAC, in morphants sprouts only turned at 9% of the somitic boundaries (Fig. 1D-E',G).

We also carried out live imaging in *plcg1^{y10}* mutants, either uninjected or injected with *netrin1a*SBMO (see Fig. S2 and Movies 1 and 2 in the supplementary material), for a period of 16.5-19 hours starting at 29-33 hpf. In control embryos (*n*=4), secondary sprouts

grew dorsally, then turned anteroposteriorly upon reaching the HMS. In *netrin 1a* morphants (*n*=3), initial dorsal growth appeared normal. However, upon reaching the HMS, the secondary sprouts usually stalled, ceasing elongation but maintaining active filopodia and failing to turn. These time-lapse data confirmed the conclusion drawn from fixed samples that *netrin 1a* morphants show specific defects in anteroposterior turning by secondary sprouts. Thus, *netrin 1a* is required specifically for secondary sprouts to turn along the HMS, but neither for their initial growth nor their dorsal elongation towards the HMS.

Netrin 1a from the MPs is responsible for PAC formation

To determine when and where Netrin 1a might act to mediate PAC formation, we examined its expression by mRNA in situ hybridization (ISH) at 22 and 32 hpf (Fig. 2A,B). Sectioning revealed *netrin 1a* labeling in the region corresponding to the MPs

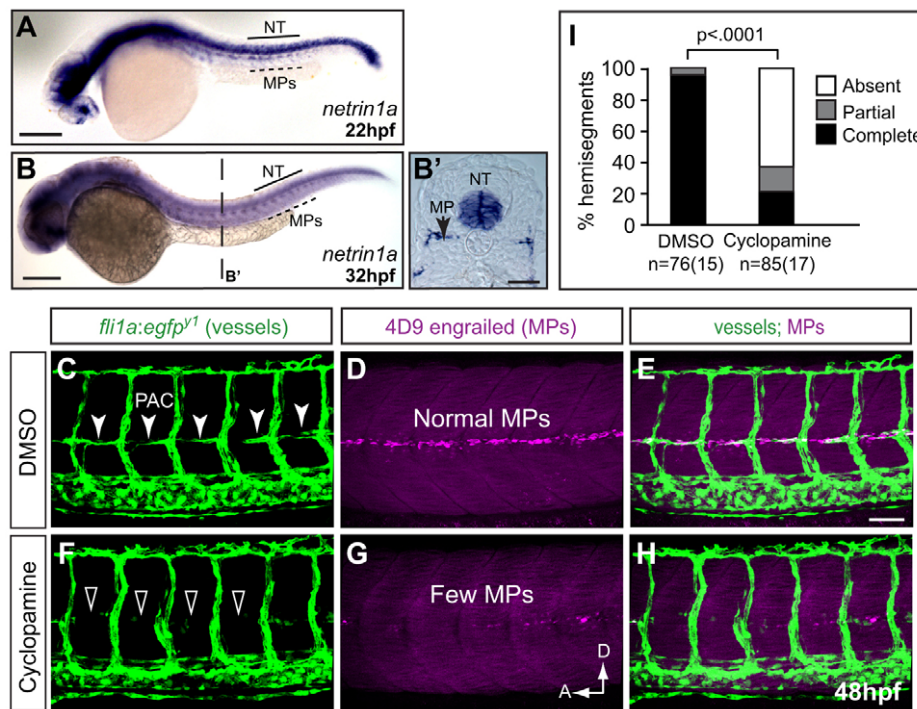


Fig. 2. Muscle pioneers express *netrin 1a* along the HMS prior to and during PAC formation and are required for PAC formation.

(A-B') mRNA in situ hybridization (ISH) shows *netrin 1a* expression in MPs and neural tube (NT) at 22 and 32 hpf. (B') Transverse section of zebrafish embryo in B at the level indicated. (C-H) The muscle pioneers (MPs) are the critical source of Netrin 1a for PAC formation. Treatment with 50 μ M cyclopamine prevents nearly all MP formation and leads to failure of PAC formation. 48 hpf *fli1a:egfp^{y1}* embryos antibody stained for vessels (GFP, green) and MPs (4D9 anti-engrailed, magenta). Confocal projections. (C-E) In DMSO-treated control embryos, MPs are present at the HMS (D) and the PAC forms normally (C, arrowheads). (F-H) In cyclopamine-treated embryos, very few MPs form (G) and the PAC is missing (F, arrowheads). (I) PAC formation was assessed in hemisegments 7-11 in DMSO-treated (97 \pm 2% complete; 3 \pm 2% partial; 0 \pm 0% absent) and cyclopamine-treated (21 \pm 6% complete; 15 \pm 4% partial; 64 \pm 7% absent) embryos. All values are mean \pm s.e.m.; *P*-value determined by Mann-Whitney U test comparing absent PACs. *n*, number of hemisegments (number of embryos). A, anterior; D, dorsal; NT, neural tube. Scale bars: 200 μ m in A-B'; 50 μ m in C-H.

at the HMS in addition to the neural tube (Fig. 2B'). Owing to their proximity, we hypothesized that the MPs are the source of the Netrin 1a that guides the PAC, and that Netrin 1a from the neural tube is irrelevant.

To test this hypothesis, we prevented MP formation by treating embryos with the Sonic hedgehog (Shh) inhibitor cyclopamine and examined PAC formation (Fig. 2C-H) (Wolff et al., 2003). We incubated *fli1a:egfp^{y1}* embryos with cyclopamine and examined the presence of MPs at 36 hpf by immunolabeling with the anti-engrailed 4D9 antibody (Wolff et al., 2003). Whereas 4D9 staining was observed at the HMS in DMSO-treated embryos, far less staining was visible in cyclopamine-treated embryos, indicating that the treatment efficiently prevented almost all MP formation. Additionally, *netrin 1a* mRNA could no longer be detected by ISH at the HMS of cyclopamine-treated embryos, whereas its expression in the neural tube was unaffected (see Fig. S3 in the supplementary material). DMSO-treated control embryos had no hemisegments missing the PAC and only 3% with a partial PAC ($n=76$ hemisegments, 15 embryos) (Fig. 2C-E,I). By contrast, in cyclopamine-treated embryos the PAC was absent in 64% of hemisegments and partially formed in 15% ($n=85$ hemisegments, 17 embryos) (Fig. 2F-I). Although cyclopamine can also affect the formation of muscles and vessels, MPs are the most sensitive cells (Wolff et al., 2003). At the carefully titrated cyclopamine dose used here the majority of the MPs are removed, but there is no visible effect on other muscles or other trunk vasculature. Since cyclopamine inhibits the formation of the source of Netrin 1a at the

HMS but does not alter *netrin 1a* expression in the spinal cord, we infer that *netrin 1a* expressed by the MPs at the HMS is the critical source of guidance information for the PAC.

To test the sufficiency of MPs for PAC formation we performed heterochronic blastula transplants (Halpern et al., 1995; Suli et al., 2006). We transplanted cells from sphere stage embryos (4 hpf) into blastula embryos (3 hpf), which allows for better targeting of the MPs. Cells from *fli1a:egfp^{y1}* donors injected with Rhodamine Dextran (RhDx) were transplanted into *fli1a:egfp^{y1}* hosts injected with *netrin1a*SBMO (Fig. 3A). RhDx-positive transplanted donor cells contributed to MPs, which were distinguished by their morphology and position at the HMS. Donor cells also contributed to the spinal cord, hypochord, fast and slow muscle cells and endothelial cells. As the donor embryos expressed *fli1a:egfp^{y1}*, endothelial cells derived from the transplanted cells were identified by RhDx and EGFP co-staining (see Fig. S4 in the supplementary material); these embryos were omitted from our analysis. Among *netrin 1a* morphant hemisegments without transplanted WT MPs, only 42% developed a complete or partial PAC (Fig. 3B-H) ($n=59$ hemisegments, 17 embryos). By contrast, 78% of hemisegments that received transplanted WT MPs developed a full or partial PAC ($n=32$ hemisegments, 17 embryos) (Fig. 3B-H). Thus, reintroducing MPs at the HMS, which presumably present the only source of Netrin 1a, is sufficient to restore PAC formation in *netrin 1a* morphants. Together with the cyclopamine experiments, this shows that MPs are the source of Netrin 1a that is responsible for secondary sprout turning at the HMS.

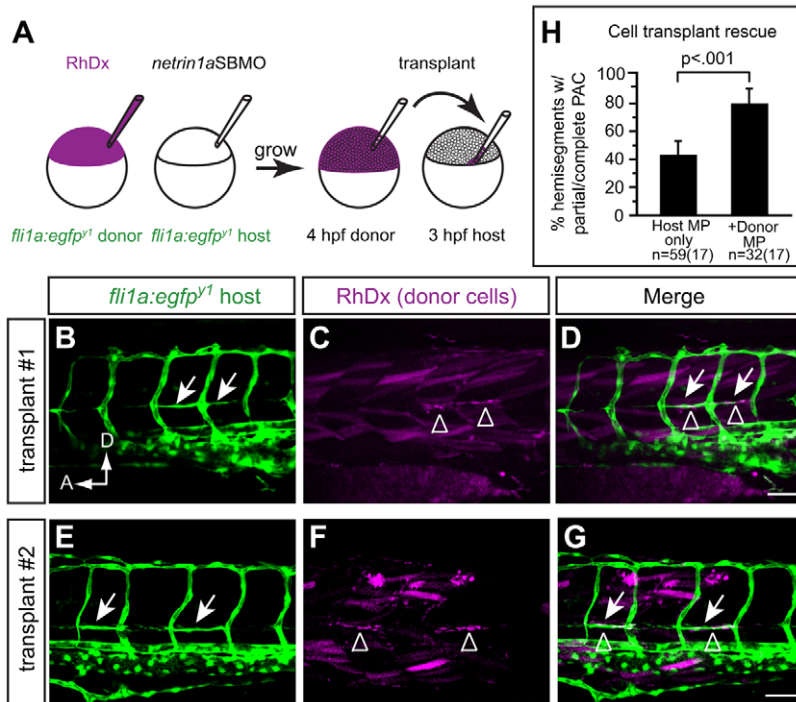


Fig. 3. Transplanting wild-type MPs at the HMS rescues PAC formation in *netrin 1a* morphants.

(A) Scheme for heterochronic transplants. Rhodamine Dextran (RhDx) is injected into one-cell stage *fli1a:egfp^{y1}* zebrafish embryos (donor). *netrin1aSBMO* is injected into one-cell stage *fli1a:egfp^{y1}* embryos (host). Cells are transferred from the RhDx embryo at 4 hpf to the *netrin1a* morphant host at 3 hpf at a location fated to include MPs. (B-G) Lateral views showing *fli1a:egfp^{y1}* and the lineage marker (RhDx) in two transplanted embryos. The PAC (arrows, B,E) forms in the same hemisegments that receive transplanted wild-type MPs (arrowheads, C,F). Confocal projections. (H) Quantitation of rescue in *netrin1a* morphants showing presence of the PAC (partial or complete) in hemisegments that either received wild-type transplanted MPs or were populated only by morphant host MPs. Host MPs only, 42±9%; transplanted donor MPs, 78±10%. All values are mean±s.e.m.; *P*-value determined by Wilcoxon signed rank test. *n*, number of hemisegments (number of embryos). A, anterior; D, dorsal; MP, muscle pioneer. Scale bar: 50 μm.

***dcc* is expressed in motoneurons and is required for attraction of secondary sprouts at the HMS and for TD formation**

There are several known Netrin 1 receptors: Deleted in colorectal cancer (*Dcc*), Neogenin, *Unc5*, Down syndrome cell adhesion molecule (*Dscam*) and integrin $\alpha6\beta4/\alpha3\beta1$ (Andrews et al., 2008; Cirulli and Yebra, 2007; Liu et al., 2009; Ly et al., 2008; Yebra et al., 2003). Of these, *Dcc* is the best studied, mediating many Netrin-dependent guidance decisions at the midline and elsewhere.

To test whether *dcc* is necessary for PAC formation, we examined PAC formation under two conditions: single morphants injected only with *plcg1SBMO*, or double morphants injected with *plcg1SBMO* and *dccTBMO* (Suli et al., 2006). Loss of *Dcc* gave defects very similar to loss of Netrin 1a: secondary sprouts formed and grew dorsally as normal, but failed to turn laterally and then anteroposteriorly to form the PAC (Fig. 4A-B'). Similar to *netrin1a* morphants, secondary sprouts formed at 90% of the intersomitic boundaries in the *plcg1 dcc* double morphants ($n=123$ hemisegments, 28 embryos). This is not significantly different from control *plcg1* morphants, where secondary sprouts formed at 97% of boundaries ($n=96$ hemisegments, 22 embryos) (Fig. 4C). However, whereas in *plcg1* single morphants only 17% of the sprouts failed to turn at the HMS, 82% of *plcg1 dcc* double-morphant sprouts failed to turn at the HMS to form a PAC (Fig. 4D). To rule out possible off-target effects of the *dccTBMO*, we co-injected *dcc* mRNA with its first few codons mutated to prevent it from being targeted by the *dccTBMO*. This mRNA rescued the PAC phenotype significantly and almost completely (Fig. 4E-G), demonstrating the specificity of the requirement for *dcc*. *netrin1a* expression and MP formation were not impaired in *dcc* morphants (see Fig. S5 in the supplementary material). Altogether, these results designate *Dcc* as a receptor required for mediating Netrin 1a signaling in regulating the turning of the secondary sprouts at the HMS to form the PAC.

We next determined whether depletion of *dcc* phenocopies the defects in TD formation. As predicted, *dcc* morphants had impaired TD formation: uninjected controls formed a partial or complete TD in 95% of the hemisegments ($n=63$ hemisegments, 21 embryos), whereas in *dcc* morphants only 45% of hemisegments had a partial or complete TD ($n=40$ hemisegments, 11 embryos) (see Fig. S1D-F in the supplementary material). Thus, *dcc* depletion indeed leads to defects in lymphatic development.

***dcc* is expressed in the central nervous system but not in endothelial cells**

To further understand how Netrin 1a-*Dcc* signaling mediates PAC formation, we examined *dcc* expression by mRNA ISH. If Netrin 1a-*Dcc* signaling acts in endothelial cells to guide them to the HMS, we would expect *dcc* expression in the secondary sprouts; however, we were unable to detect *dcc* mRNA in any endothelial cells. Instead, *dcc* is expressed in the brain and ventral spinal cord at 22 and 32 hpf (Fig. 5A,B). These results suggest that Netrin 1a-*Dcc*-mediated guidance of these sprouts is not endothelial cell autonomous but instead might be acting through neurons. Since Netrin-*Dcc* signaling is known to mediate axon guidance in many contexts, we hypothesized that in the zebrafish trunk it guides axons that in turn are necessary for PAC formation. If so, we would expect neurons with axons close to the HMS to express *dcc* prior to PAC formation. Single-cell dye labeling has shown that rostral primary motoneuron (RoP) axons extend ventrally along the center of the hemisegment, then turn along the HMS as early as 24 hpf (Eisen et al., 1986), with SMN axons following shortly thereafter. Other primary motoneurons include the caudal primary motoneurons (CaPs) and middle primary motoneurons (MiPs), named for their relative cell body positions in the spinal cord (Fig. 5C,D; Fig. 6A). At 55 hpf, we confirmed that the HMS is contacted by motoneuron axons (Fig. 5D). To determine if these motoneurons express *dcc*, we double labeled *hb9:GFP* embryos with anti-GFP

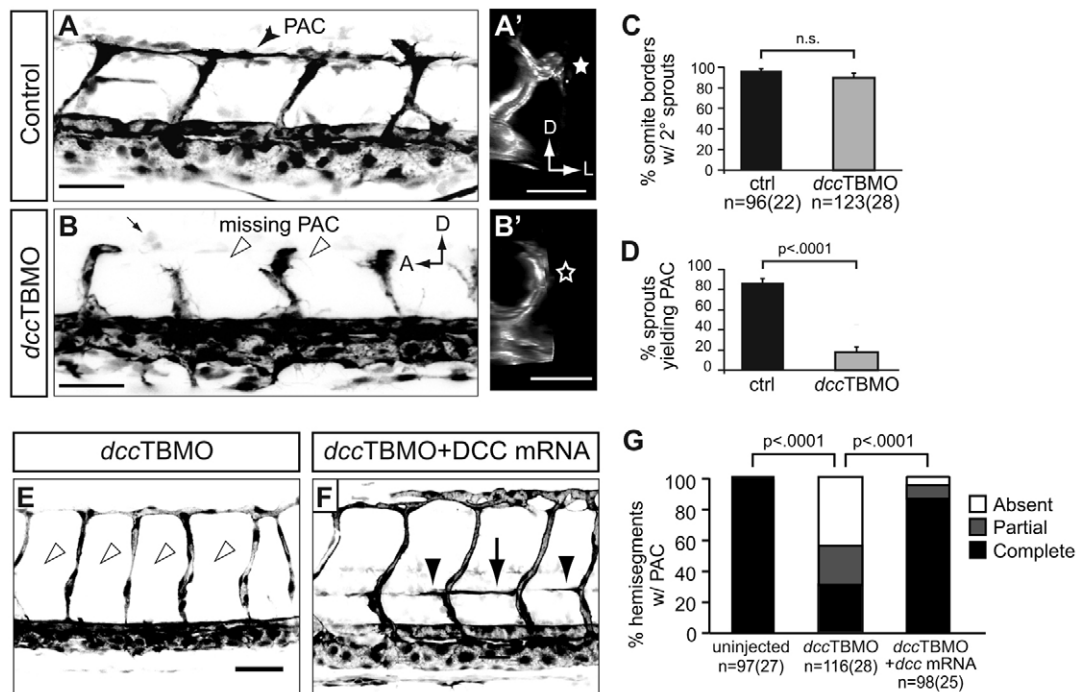


Fig. 4. *dcc* is required for turning of secondary sprouts at the HMS and injection of *dcc* mRNA rescues PAC formation in *dcc* morphants. (A-B') 48 hpf *fli1a:egfp^{v1}* zebrafish embryos injected with (A,A') *plcg1* splice-blocking MO (*plcg1*SBMO) only (control) or (B,B') *plcg1*SBMO plus *dcc* translation-blocking MO (*dcc*TBMO). (A) Lateral view. In *plcg1* morphants, secondary sprouts grow from the PCV and turn at the HMS to form the PAC (arrowhead). (A') Transverse volume rendering of A showing mediolateral turn of secondary sprout. (star). (B) Lateral view. In embryos co-injected with *plcg1*SBMO and *dcc*TBMO, secondary sprouts form but fail to turn and form the PAC (arrowheads). (B') Transverse volume rendering of B showing failure of secondary sprout to turn laterally (star). (C) Secondary sprouts formed from the PCV were counted in 4-5 intersomitic boundaries per embryo between segments 7-11 in *plcg1* single morphants (control, 97±3%) and in *plcg1*SBMO/*dcc*TBMO double morphants (*dcc*TBMO, 90±5%), and showed no significant difference (n.s.). (D) Secondary sprouts that turned to form the PAC were counted in *plcg1* single morphants (87±5%) and *plcg1*/*dcc* double morphants (18±5%), which showed greatly reduced turning in the absence of Dcc. (E,F) Lateral views of 48 hpf *fli1a:egfp^{v1}* embryos injected with (E) *dcc*TBMO or (F) *dcc*TBMO and *dcc* mRNA. The PAC is absent in *dcc* morphants (E, arrowheads) and restored when *dcc* morphants are co-injected with *dcc* mRNA (F, arrow and arrowheads indicate complete and partial rescue, respectively). (G) Quantification of complete, partial or absent PAC. Uninjected: complete, 99±1%; partial, 1±1%; absent, 0±0%. *dcc* morphant: complete, 31±7%; partial, 25±6%; absent, 44±7%. *dcc* morphant + RNA: complete, 86±5%; partial, 9±4%; absent, 5±3%. All values are mean±s.e.m.; error bars show s.e.m.; P-value determined by Mann-Whitney U test (comparing absent PACs in G). n, number of hemisegments (number of embryos). A, anterior; D, dorsal; L, lateral; PAC, parachordal chain. Scale bars: 50 μm.

and performed ISH for the *dcc* transcript. Longitudinal sections of these embryos reveal clear localization of *dcc* mRNA in the cell bodies of primary motoneurons, and of RoP in particular (Fig. 5C).

***netrin 1a* and *dcc* morphants do not form axons at the HMS**

Our hypothesis that Netrin 1a-Dcc signaling controls PAC formation indirectly through motoneuron axon guidance predicts these axons to be absent in *netrin 1a* and *dcc* morphants. We injected *netrin 1a* or *dcc* MOs into *hb9:GFP* transgenic embryos. Embryos were imaged at 55 hpf, when the axon fascicle at the HMS, which consists of RoP and secondary motor axons, is reliably visible in this transgenic line. Motoneuron axons were present at the HMS in 98% of uninjected control hemisegments ($n=97$ hemisegments, 32 embryos), but far less often in morphants: 27% of hemisegments in *netrin 1a* morphants ($n=80$ hemisegments, 20 embryos) and 51% of hemisegments in *dcc* morphants ($n=63$ hemisegments, 22 embryos) (Fig. 6B-D). Thus, *netrin 1a* and *dcc* are necessary for primary and secondary motor axon formation at the HMS.

Genetic disruption or laser ablation of motoneurons causes loss of the PAC

To directly test whether motoneuron axons at the HMS are crucial for PAC formation, we inhibited motoneuron formation by knocking down *olig2*, a basic helix-loop-helix (bHLH) transcription factor that is necessary for the development of motoneurons and oligodendrocytes (Lu et al., 2002; Park et al., 2002; Zhou and Anderson, 2002). We confirmed the published observation that *olig2* morphants do not form motor axons (Park et al., 2002) and then scored embryos for the PAC. The PAC was absent in only 6% of uninjected control hemisegments ($n=71$ hemisegments, 23 embryos), whereas in the *olig2* morphants the PAC was absent in 40% of hemisegments ($n=166$ hemisegments, 48 embryos) (Fig. 7A-F,J). We also found that injection of MOs targeting *islet1* (*islet1*), a gene necessary for motoneuron differentiation (Hutchinson and Eisen, 2006), also results in an absence of motoneurons and in a PAC defect, a phenotype also seen in *islet1* mutants (see Fig. S6 in the supplementary material). *islet1* morphants formed MPs normally and expressed *netrin 1a* at the HMS (see Fig. S5 in the supplementary material). Taken together these data provide strong evidence that motor axons are crucial for PAC formation.

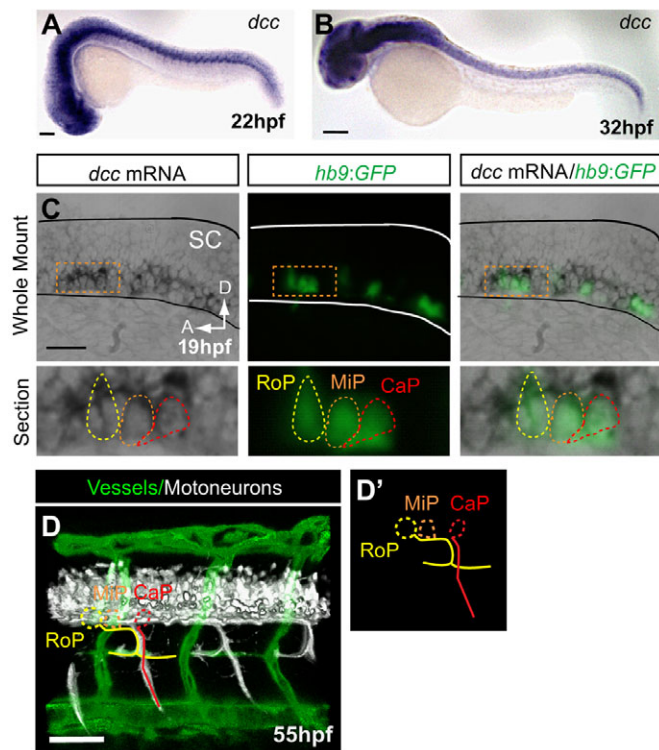


Fig. 5. *dcc* is not detected in endothelial secondary sprouts but is expressed in motoneurons with axons present at the HMS prior to PAC formation. (A,B) *dcc* mRNA is expressed in the ventral spinal cord at 22 and 32 hpf and is not detectable in the secondary sprouts or other trunk vasculature. (C) Whole-mount and longitudinal section of *hb9:GFP* transgenic zebrafish embryo showing *dcc* mRNA ISH (purple), where *hb9:GFP* labels only motoneurons at early stages (green). (D) Lateral volume rendering of *fli1a:dsRedEx; hb9:GFP* embryo at 55 hpf. Double transgenic labels endothelial cells (green) and motoneuron axons (white) in the trunk. Rostral primary motoneuron (RoP, yellow) axons are present at the HMS adjacent to the PAC. (D') Outline of motoneurons alone. CaP, caudal primary motoneuron (red); MiP, middle primary motoneuron (orange; axon omitted for clarity). SC, spinal cord; A, anterior; D, dorsal. Scale bars: 100 μ m.

Finally, we used laser ablation to specifically prevent motoneuron axon formation. We targeted motoneuron cell bodies in a single somite of *hb9:KikGR; fli1a:egfp^{v1}* zebrafish embryos (Fig. 7G-I). Since the fine motor axon fascicle at the HMS is not always visible in the *hb9:KikGR* line, we used the CaP axon fascicle projection as a measure of successful motoneuron ablation. Whereas SMNs can pathfind normally (albeit with a delay) after ablation of primary motoneurons (Pike et al., 1992), in successfully ablated segments we saw no secondary motor axons. We analyzed 29 laser-ablated embryos (81 hemisegments) in which the primary and secondary motoneuron axons were completely absent, discarding hemisegments in which the ablation was unsuccessful or partial. Among the 65 hemisegments in which the motoneurons were untreated and formed normally, only 5% had an absent PAC. By contrast, of the 16 hemisegments in which the CaP motoneuron was successfully ablated, 50% had an absent PAC (Fig. 7K). These results provide direct evidence that motoneurons are essential for PAC formation. Additionally, the less penetrant phenotype observed in *olig2* morphants and laser-ablated embryos compared

with the *netrin 1a* and *dcc* morphants suggests that *netrin 1a* might act through both motoneuron-dependent and -independent pathways in PAC formation.

DISCUSSION

Our study demonstrates that *netrin 1a* expressed by MPs guides *dcc*-expressing RoP motoneuron axons and associated secondary motor axons to extend along the HMS. These axons at the HMS are required for secondary sprouts to turn, form the PAC, and ultimately develop into the zebrafish lymphatic system. In contrast to previous reports, including our own (Wilson et al., 2006), that focus on Netrin signaling directly to the endothelium to promote or inhibit angiogenesis (Bouvier et al., 2008; Epting et al., 2010; Larrivee et al., 2007; Lu et al., 2004; Park et al., 2004; Wilson et al., 2006), our data support an alternative model whereby *netrin 1a* guides endothelial cells indirectly, via motor axons. This report defines a novel *in vivo* role for Netrin, which was one of the first neural guidance cues identified, as essential to lymphatic vascular pathfinding and development through its function as an axonal pathfinding cue. We provide *in vivo* evidence that motor axons are required for endothelial cell guidance. Although it has been shown that motor axons are required for the expression of arterial and smooth muscle markers (Mukoyama et al., 2005), to the best of our knowledge this is the first demonstration of a direct requirement for axons in vascular guidance and lymphangiogenesis.

netrin 1a mRNA is expressed by the MPs from ~15 hpf through 32 hpf at the HMS (Fig. 2A-B') (Lauderdale et al., 1997). Our cyclopamine and transplantation experiments underscore the necessary and sufficient role of MPs and their expression of *netrin 1a* at the HMS in the ultimate formation of the zebrafish lymphatic system (Figs 2, 3 and see Fig. S1 in the supplementary material). The spatiotemporal expression pattern of *netrin 1a* is coincident with two important events at the HMS: first, motoneuron axon elongation at the HMS at 24 hpf; second, the turning of the secondary sprouts at the HMS to form the PAC, which occurs at ~36 hpf.

We knocked down the Netrin receptor Dcc and showed that the resulting vascular defect phenocopied the *netrin 1a* morphant (Fig. 4). This shared phenotype is characterized by secondary sprouts that fail to turn at the HMS, form a PAC and develop a lymphatic system. However, we were unable to detect *dcc* expression in secondary sprouts by mRNA ISH (Fig. 5). This lack of *dcc* expression in endothelial cells is consistent with previous findings that *dcc* is mostly expressed in the central nervous system (Fricke and Chien, 2005; Gad et al., 1997). The absence of vascular *dcc* expression challenged our initial model in which Dcc mediates a direct pro-angiogenic effect of Netrin 1a, and led us to consider an alternative model. *dcc* is prominently expressed in RoP motoneurons, which project axons laterally and then along the HMS prior to PAC formation (Fig. 5). We therefore hypothesized that *dcc*-expressing RoP motoneuron axons course along the HMS, guided by their attraction to Netrin 1a produced by MPs, and that they, together with the SMNs that follow them, are crucial for directing the endothelial tips of the secondary sprouts to turn and form the PAC. We also recognize that Dcc is one of several Netrin receptors, and do not exclude the possibility that Netrin has a direct effect on the endothelial cells through an as yet undetermined receptor.

Consistent with this alternative model, motoneurons fail to elongate axons along the HMS in both *netrin 1a* and *dcc* morphants (Fig. 6). To demonstrate that motoneurons are crucial for PAC

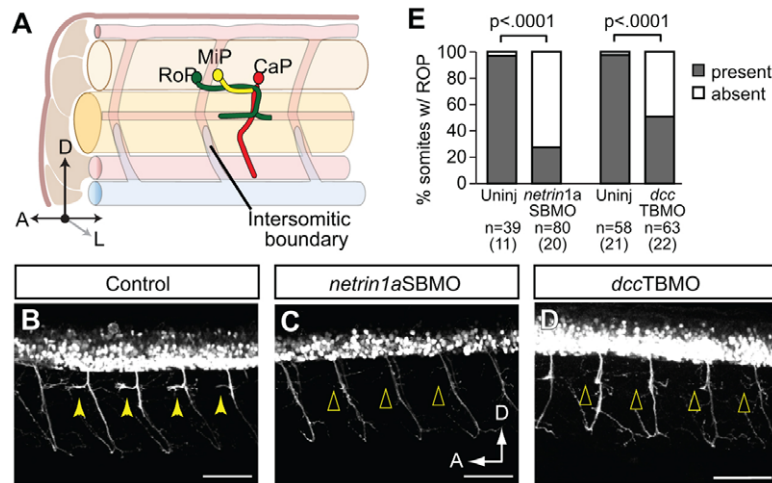


Fig. 6. RoP axons and associated secondary axons at the HMS do not form in *netrin 1a* and *dcc* morphants. (A) Diagram of RoP, middle primary (MiP) and caudal primary (CaP) axons at 36 hpf. (B-D) Lateral view of 55 hpf *hb9:GFP* zebrafish embryos injected with (B) no MO, (C) *netrin 1a* splice-blocking MO (*netrin1aSBMO*) or (D) *dcc* translation-blocking MO (*dccTBMO*). Confocal projections. (B) Uninjected controls show axons at the HMS in almost every somite (arrowheads). In embryos injected with (C) *netrin1aSBMO* or (D) *dccTBMO*, axons fail to form at the HMS (arrowheads). (E) Axons at the HMS were counted in 3-4 somites per embryo in segments 7-11 in control, *netrin1aSBMO*- and *dccTBMO*-injected embryos. Uninjected, 97±3%; *netrin 1a* morphant, 27±7%. Uninjected, 98±2%; *dcc* morphant, 49±7%. All values are mean±s.e.m.; *P*-value determined by Mann-Whitney U test. *n*, number of hemisegments (number of embryos). A, anterior; D, dorsal; L, lateral; RoP, rostral primary motoneuron; MiP, middle primary motoneuron; CaP, caudal primary motoneuron. Scale bars: 50 μm.

formation, we disrupted motoneurons in a *netrin 1a*- and *dcc*-independent fashion. After disrupting motoneurons by *olig2* or *isll* knockdown or laser ablation, secondary sprouts failed to make the turn along the HMS and form the PAC. Note that SMNs project out of the spinal cord a few hours after RoP and other primary motoneurons, with some of their axons fasciculating with the RoP

axon, likely innervating the HMS. Since we are unable to distinguish the behavior of the SMN axons from that of RoP, it is possible that other axons in the RoP fascicle contribute to PAC formation. Thus, MPs and motor axons act in concert to alter the mediolateral and anteroposterior trajectory of secondary sprouts and guide them along the HMS.

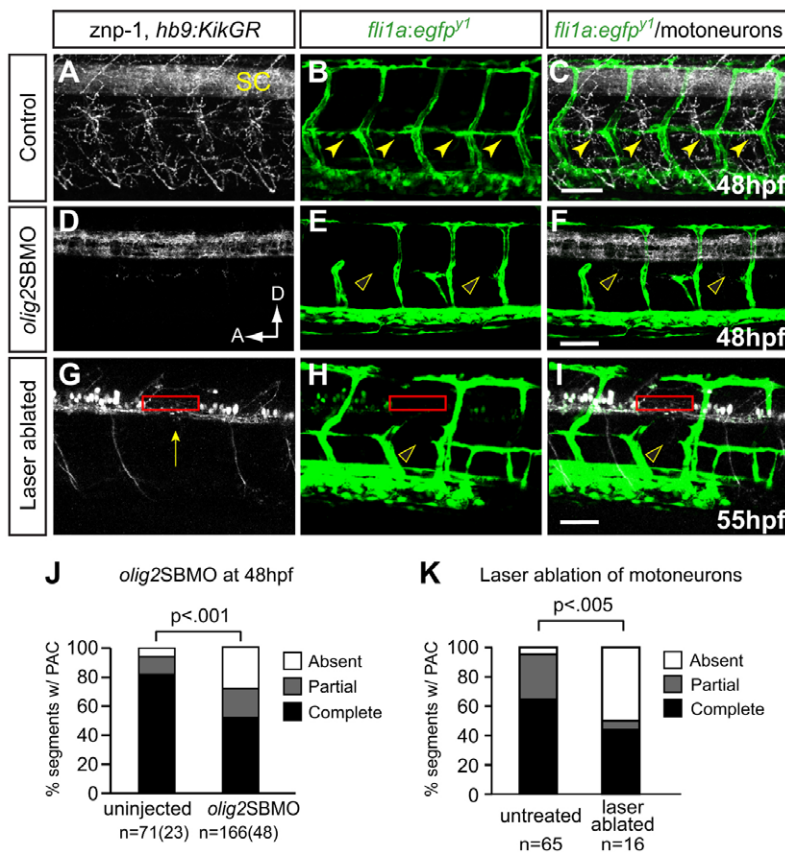


Fig. 7. Preventing differentiation or laser ablation of motoneurons prevents PAC formation. (A-F) Lateral views of 48 hpf *fli1a:egfp^{Y1}* zebrafish embryos either uninjected or injected with *olig2* splice-blocking MO (*olig2SBMO*) showing labeled vessels (green) and neurons (*znp-1* antibody, white). Confocal projection. (A) Motor axons grow ventrally from the spinal cord (SC) in controls. (B,C) The PAC forms normally in controls (arrowheads). (D) Motoneurons and their axons are absent in *olig2* morphants. (E,F) PAC does not form in *olig2* morphants (arrowheads). (G-I) Lateral view of 55 hpf *fli1a:egfp^{Y1}*; *hb9:KikGR* after photoconversion, with vessels in green and motoneurons in white. Confocal projections. Motoneuron cell bodies were targeted by laser in one somite per embryo (red rectangle), resulting in ablation of motoneurons, (G) missing caudal primary motoneuron (CaP) axon (arrow), and (H,I) missing PAC (arrowhead) in that somite. (J) The PAC was scored in 4-5 somites per embryo in uninjected control embryos (complete, 82±6%; partial, 12±6%; absent, 6±4%) and *olig2* morphants (complete, 52±5%; partial, 20±3%; absent, 28±4%). All values are mean±s.e.m.; *P*-value determined by Mann-Whitney U test. *n*, number of hemisegments (number of embryos). (K) The number of somites with PACs was quantified in somites that were untreated or successfully laser ablated. Untreated: complete or partial, 95%; absent, 5%. Ablated: complete or partial, 50%; absent, 50%. *n*, number of hemisegments; *P*-value determined by Fischer's exact test. A, anterior; D, dorsal. Scale bars: 50 μm.

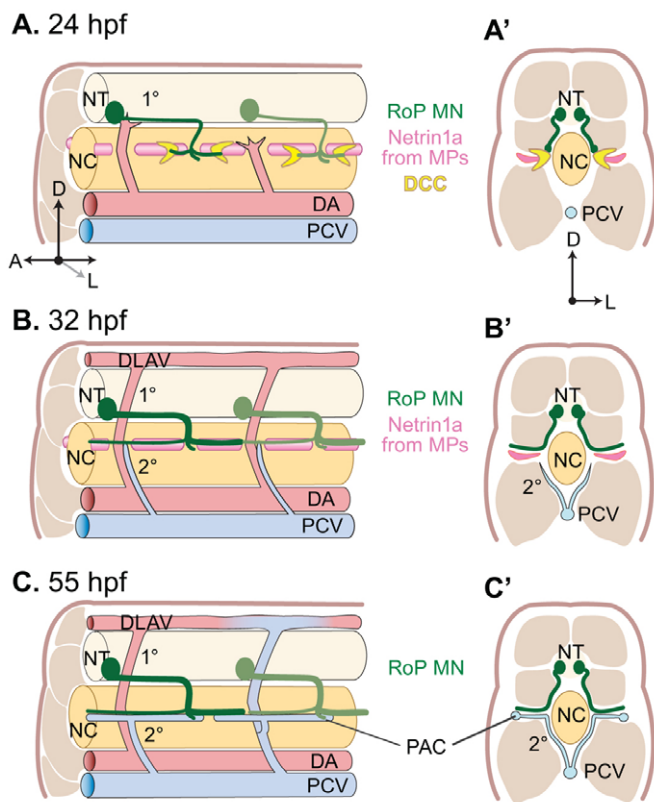


Fig. 8. Model of motoneuron axons and PAC formation.

(A-C') Oblique lateral view [A-C, for clarity only the rostral primary motoneuron (RoP) is shown] and transverse view [A'-C', dorsal aorta (DA) and primary sprouts omitted for clarity] of zebrafish trunk. (A,A') RoP motoneuron axons (green) expressing *dcc* (yellow) exit the spinal cord and extend ventrally towards the HMS at 24 hpf. *netrin 1a* (pink) is expressed by the MPs before and during motoneuron axon pathfinding. (B,B') *netrin 1a* expressed by MPs and *dcc* expressed by motoneuron axons are necessary for axon extension along the horizontal myoseptum (HMS). Secondary sprouts (blue) grow dorsally to the HMS. (C,C') The axons at the HMS are required for secondary sprouts to grow laterally at the HMS and then turn anteriorly and posteriorly along the HMS to form the PAC. A, anterior; D, dorsal; L, lateral; MPs, muscle pioneers; DLAV, dorsal longitudinal anastomotic vessel; PCV, posterior cardinal vein; PAC, parachordal chain; NT, neural tube; NC, notochord; 1°, primary sprouts; 2°, secondary sprouts.

We are not aware of any other instance in which a prototypic guidance cue, such as Netrin, is crucial for guiding axons, the subsequent trajectory of which plays an essential function in vascular pathfinding or lymphangiogenesis *in vivo*. We note that our group and others have proposed direct effects of Netrins on the vascular and lymphatic endothelium in cell culture experiments and in mouse and zebrafish studies (Bouvree et al., 2008; Larrivee et al., 2007; Lauderdale et al., 1997; Park et al., 2004; Wilson et al., 2006). One report suggests an endothelial cell-autonomous role for Netrin 1a-Unc5b signaling in promoting PAC formation (Epting et al., 2010). Since the PAC fails to form in 50% of hemisegments where the motoneuron axon has been ablated, but forms even less often in *netrin 1a* and *dcc* morphants, we do not exclude the possibility that Netrin 1a might have an additional direct effect on the endothelium of secondary sprouts via a non-Dcc receptor.

We have considered the molecular basis by which axons might provide crucial instructions for PAC formation and lymphangiogenesis (Fig. 8). Multiple permutations of potential interactions between the MPs, the RoP motoneuron axons and the endothelium of secondary sprouts are possible. For example, axons may provide either paracrine or juxtacrine cues that have direct effects on the endothelium, or induce MPs to express such endothelial factors. Without knowing whether the requirement for the axonal contribution at the HMS is a direct interaction with the endothelium or an indirect interaction with MPs, it is challenging to devise a rational cellular or biochemical strategy to systematically identify the crucial cell-cell interactions and the molecules that mediate these interactions. Given the essential role of PAC formation in lymphangiogenesis, as emphasized in this study (see Fig. S1 in the supplementary material), and the ease of scoring a loss-of-function phenotype, ongoing mutagenesis screens and future identification of the genes involved might provide valuable insight.

Reports from others have begun to identify the genetic basis for zebrafish with defective lymphangiogenesis (Geudens et al., 2010; Hermans et al., 2010; Hogan et al., 2009a; Hogan et al., 2009b; Kuchler et al., 2006). Most describe zebrafish mutants or morphants that have defects in the earliest step of lymphangiogenesis: secondary sprout formation. This process remains conspicuously intact in the absence of *netrin 1a*, *dcc* or RoP motoneurons. One report implicates Notch signaling as necessary for venous-to-lymphatic differentiation; when Notch signaling is reduced, PAC formation appears to be specifically inhibited (Geudens et al., 2010). This phenotype is strikingly similar to that we observe in the absence of motoneuron axons, in which secondary sprouts form from the PCV but do not turn at the HMS. These investigators suggested that Notch signaling disrupts venous-lymphatic specification, causing flow reversal in the primary sprouts. We found no evidence of flow reversal in the primary sprouts in our case, indicating that the failure of turning is not due to an absence of venous-lymphatic specification.

Our original interest in Netrin signaling and zebrafish lymphangiogenesis was stimulated by the desire to examine whether Netrins were a direct attractive lymphangiogenic cue. Our group has previously shown that Netrin 4 induces lymphangiogenesis in mammalian systems and potentially mediates this effect by directly activating $\alpha 6 \beta 1$ integrin receptor expressed by endothelial cells (Larrieu-Lahargue et al., 2010; Larrieu-Lahargue et al., 2011). Although we find that Netrins are required as a positive stimulator of PAC formation and lymphangiogenesis, this study led us to recognize that the requirement for Netrin 1a-Dcc signaling in lymphangiogenesis is through its originally described role as a mediator of axon pathfinding. Furthermore, we implicate Netrin 1a-Dcc signaling in a novel guidance mechanism wherein axons mediate vascular growth.

Acknowledgements

We thank D. Lim for graphical assistance; Hideo Otsuna for help with FluorRender; K. Thomas, F. Poulain, N. London, K. Kwan and A. Chan for critical reading of this manuscript; S. Hutchinson, L. Hale and J. Eisen for helpful discussions; G. King and the Centralized Zebrafish Animal Resource Facility; C. Rodesch, K. Carney and the Cell Imaging Core; Xiaoming Sheng at the Biostatistics Core for help with statistical analysis; M. Granato, J. Yost and N. Lawson for fish; L. Hale and J. Eisen for *isl1* morpholinos; B. Appel for *olig2* morpholino; Uwe Strähle for a partial *netrin 1a* clone; and M. Juryneć and D. Grunwald for the 4D9 antibody and cyclopamine. Funding: D.Y.L. and C.-B.C., NHLBI; B.W., Intramural Research Program of the NIH (NICHD). Deposited in PMC for release after 12 months.

Competing interests statement

The authors declare no competing financial interests.

Supplementary material

Supplementary material for this article is available at <http://dev.biologists.org/lookup/suppl/doi:10.1242/dev.068403/-DC1>

References

- Adams, R. H. and Eichmann, A. (2010). Axon guidance molecules in vascular patterning. *Cold Spring Harb. Perspect. Biol.* **2**, a001875.
- Andrews, G. L., Tanglao, S., Farmer, W. T., Morin, S., Brotman, S., Berberoglu, M. A., Price, H., Fernandez, G. C., Mastick, G. S., Charron, F. et al. (2008). Dscam guides embryonic axons by Netrin-dependent and -independent functions. *Development* **135**, 3839-3848.
- Bates, D., Taylor, G. I., Minichiello, J., Farlie, P., Cichowitz, A., Watson, N., Klagsbrun, M., Mamluk, R. and Newgreen, D. F. (2003). Neurovascular congruence results from a shared patterning mechanism that utilizes Semaphorin3A and Neuropilin-1. *Dev. Biol.* **255**, 77-98.
- Beattie, C. E. (2000). Control of motor axon guidance in the zebrafish embryo. *Brain Res. Bull.* **53**, 489-500.
- Bedell, V. M., Yeo, S. Y., Park, K. W., Chung, J., Seth, P., Shivalingappa, V., Zhao, J., Obara, T., Sukhatme, V. P., Drummond, I. A. et al. (2005). roundabout4 is essential for angiogenesis in vivo. *Proc. Natl. Acad. Sci. USA* **102**, 6373-6378.
- Bouvier, K., Larrivee, B., Lv, X., Yuan, L., DeLafarge, B., Freitas, C., Mathivet, T., Breant, C., Tessier-Lavigne, M., Bikfalvi, A. et al. (2008). Netrin-1 inhibits sprouting angiogenesis in developing avian embryos. *Dev. Biol.* **318**, 172-183.
- Bussmann, J., Bos, F. L., Urasaki, A., Kawakami, K., Duckers, H. J. and Schulte-Merker, S. (2010). Arteries provide essential guidance cues for lymphatic endothelial cells in the zebrafish trunk. *Development* **137**, 2653-2657.
- Carmeliet, P. and Tessier-Lavigne, M. (2005). Common mechanisms of nerve and blood vessel wiring. *Nature* **436**, 193-200.
- Castets, M., Coissieux, M. M., Delloye-Bourgeois, C., Bernard, L., Delcros, J. G., Bernet, A., Laudet, V. and Mehlen, P. (2009). Inhibition of endothelial cell apoptosis by netrin-1 during angiogenesis. *Dev. Cell* **16**, 614-620.
- Cirulli, V. and Yebra, M. (2007). Netrins: beyond the brain. *Nat. Rev. Mol. Cell Biol.* **8**, 296-306.
- Dickson, B. J. (2002). Molecular mechanisms of axon guidance. *Science* **298**, 1959-1964.
- Eisen, J. S., Myers, P. Z. and Westerfield, M. (1986). Pathway selection by growth cones of identified motoneurons in live zebrafish embryos. *Nature* **320**, 269-271.
- Epting, D., Wendik, B., Bennewitz, K., Dietz, C. T., Driever, W. and Kroll, J. (2010). The Rac1 regulator ELMO1 controls vascular morphogenesis in zebrafish. *Circ. Res.* **107**, 45-55.
- Flanagan-Steet, H., Fox, M. A., Meyer, D. and Sanes, J. R. (2005). Neuromuscular synapses can form in vivo by incorporation of initially aneural postsynaptic specializations. *Development* **132**, 4471-4481.
- Fricke, C. and Chien, C. B. (2005). Cloning of full-length zebrafish dcc and expression analysis during embryonic and early larval development. *Dev. Dyn.* **234**, 732-739.
- Furne, C., Rama, N., Corset, V., Chedotal, A. and Mehlen, P. (2008). Netrin-1 is a survival factor during commissural neuron navigation. *Proc. Natl. Acad. Sci. USA* **105**, 14465-14470.
- Gad, J. M., Keeling, S. L., Wilks, A. F., Tan, S. S. and Cooper, H. M. (1997). The expression patterns of guidance receptors, DCC and Neogenin, are spatially and temporally distinct throughout mouse embryogenesis. *Dev. Biol.* **192**, 258-273.
- Geudens, I., Herpers, R., Hermans, K., Segura, I., Ruiz de Almodovar, C., Bussmann, J., De Smet, F., Vandeveld, W., Hogan, B. M., Siekmann, A. et al. (2010). Role of delta-like-4/Notch in the formation and wiring of the lymphatic network in zebrafish. *Arterioscler. Thromb. Vasc. Biol.* **30**, 1695-1702.
- Halpern, M. E., Thisse, C., Ho, R. K., Thisse, B., Riggleman, B., Trevarrow, B., Weinberg, E. S., Postlethwait, J. H. and Kimmel, C. B. (1995). Cell-autonomous shift from axial to paraxial mesodermal development in zebrafish floating head mutants. *Development* **121**, 4257-4264.
- Hermans, K., Claes, F., Vandeveld, W., Zheng, W., Geudens, I., Orsenigo, F., De Smet, F., Gjini, E., Anthonis, K., Ren, B. et al. (2010). Role of synectin in lymphatic development in zebrafish and frogs. *Blood* **116**, 3356-3366.
- Hogan, B. M., Bos, F. L., Bussmann, J., Witte, M., Chi, N. C., Duckers, H. J. and Schulte-Merker, S. (2009a). Ccbe1 is required for embryonic lymphangiogenesis and venous sprouting. *Nat. Genet.* **41**, 396-398.
- Hogan, B. M., Herpers, R., Witte, M., Helotera, H., Alitalo, K., Duckers, H. J. and Schulte-Merker, S. (2009b). Vegf/Flt4 signalling is suppressed by Dll4 in developing zebrafish intersegmental arteries. *Development* **136**, 4001-4009.
- Hong, K., Hinck, L., Nishiyama, M., Poo, M. M., Tessier-Lavigne, M. and Stein, E. (1999). A ligand-gated association between cytoplasmic domains of UNC5 and DCC family receptors converts netrin-induced growth cone attraction to repulsion. *Cell* **97**, 927-941.
- Hutchinson, S. A. and Eisen, J. S. (2006). Islet1 and Islet2 have equivalent abilities to promote motoneuron formation and to specify motoneuron subtype identity. *Development* **133**, 2137-2147.
- Kuchler, A. M., Gjini, E., Peterson-Maduro, J., Cancilla, B., Wolburg, H. and Schulte-Merker, S. (2006). Development of the zebrafish lymphatic system requires VEGFC signaling. *Curr. Biol.* **16**, 1244-1248.
- Kwan, K. M., Fujimoto, E., Grabher, C., Mangum, B. D., Hardy, M. E., Campbell, D. S., Parant, J. M., Yost, H. J., Kanki, J. P. and Chien, C. B. (2007). The Tol2kit: a multisite gateway-based construction kit for Tol2 transposon transgenesis constructs. *Dev. Dyn.* **236**, 3088-3099.
- Larrieu-Lahargue, F., Welm, A. L., Thomas, K. R. and Li, D. Y. (2010). Netrin-4 induces lymphangiogenesis in vivo. *Blood* **115**, 5418-5426.
- Larrieu-Lahargue, F., Welm, A. L., Thomas, K. R. and Li, D. Y. (2011). Netrin-4 activates endothelial integrin $\alpha 6 \beta 1$. *Circ. Res.* (in press).
- Larrivee, B., Freitas, C., Trombe, M., Lv, X., Delafarge, B., Yuan, L., Bouvier, K., Breant, C., Del Toro, R., Brechot, N. et al. (2007). Activation of the UNC5B receptor by Netrin-1 inhibits sprouting angiogenesis. *Genes Dev.* **21**, 2433-2447.
- Larrivee, B., Freitas, C., Suchting, S., Brunet, I. and Eichmann, A. (2009). Guidance of vascular development: lessons from the nervous system. *Circ. Res.* **104**, 428-441.
- Lauderdale, J. D., Davis, N. M. and Kuwada, J. Y. (1997). Axon tracts correlate with netrin-1a expression in the zebrafish embryo. *Mol. Cell. Neurosci.* **9**, 293-313.
- Lawson, N. D., Mugford, J. W., Diamond, B. A. and Weinstein, B. M. (2003). phospholipase C gamma-1 is required downstream of vascular endothelial growth factor during arterial development. *Genes Dev.* **17**, 1346-1351.
- Lejmi, E., Leconte, L., Pedron-Mazoyer, S., Ropert, S., Raoul, W., Lavalette, S., Bouras, I., Feron, J. G., Maitre-Boube, M., Assayag, F. et al. (2008). Netrin-4 inhibits angiogenesis via binding to neogenin and recruitment of UNC5B. *Proc. Natl. Acad. Sci. USA* **105**, 12491-12496.
- Liu, G., Li, W., Wang, L., Kar, A., Guan, K. L., Rao, Y. and Wu, J. Y. (2009). DSCAM functions as a netrin receptor in commissural axon pathfinding. *Proc. Natl. Acad. Sci. USA* **106**, 2951-2956.
- Lu, Q. R., Sun, T., Zhu, Z., Ma, N., Garcia, M., Stiles, C. D. and Rowitch, D. H. (2002). Common developmental requirement for Olig function indicates a motor neuron/oligodendrocyte connection. *Cell* **109**, 75-86.
- Lu, X., Le Noble, F., Yuan, L., Jiang, Q., De Lafarge, B., Sugiyama, D., Breant, C., Claes, F., De Smet, F., Thomas, J. L. et al. (2004). The netrin receptor UNC5B mediates guidance events controlling morphogenesis of the vascular system. *Nature* **432**, 179-186.
- Ly, A., Nikolaev, A., Suresh, G., Zheng, Y., Tessier-Lavigne, M. and Stein, E. (2008). DSCAM is a netrin receptor that collaborates with DCC in mediating turning responses to netrin-1. *Cell* **133**, 1241-1254.
- Makita, T., Suvov, H. M., Garipey, C. E., Yanagisawa, M. and Ginty, D. D. (2008). Endothelins are vascular-derived axonal guidance cues for developing sympathetic neurons. *Nature* **452**, 759-763.
- Melani, M. and Weinstein, B. M. (2009). Common factors regulating patterning of the nervous and vascular systems. *Annu. Rev. Cell Dev. Biol.* **26**, 639-665.
- Mukoyama, Y. S., Gerber, H. P., Ferrara, N., Gu, C. and Anderson, D. J. (2005). Peripheral nerve-derived VEGF promotes arterial differentiation via neuropilin 1-mediated positive feedback. *Development* **132**, 941-952.
- Navankasattusas, S., Whitehead, K. J., Suli, A., Sorensen, L. K., Lim, A. H., Zhao, J., Park, K. W., Wythe, J. D., Thomas, K. R., Chien, C. B. et al. (2008). The netrin receptor UNC5B promotes angiogenesis in specific vascular beds. *Development* **135**, 659-667.
- Park, H. C., Mehta, A., Richardson, J. S. and Appel, B. (2002). olig2 is required for zebrafish primary motor neuron and oligodendrocyte development. *Dev. Biol.* **248**, 356-368.
- Park, K. W., Crouse, D., Lee, M., Karnik, S. K., Sorensen, L. K., Murphy, K. J., Kuo, C. J. and Li, D. Y. (2004). The axonal attractant Netrin-1 is an angiogenic factor. *Proc. Natl. Acad. Sci. USA* **101**, 16210-16215.
- Pike, S. H. and Eisen, J. S. (1990). Identified primary motoneurons in embryonic zebrafish select appropriate pathways in the absence of other primary motoneurons. *J. Neurosci.* **10**, 44-49.
- Pike, S. H., Melancon, E. F. and Eisen, J. S. (1992). Pathfinding by zebrafish motoneurons in the absence of normal pioneer axons. *Development* **114**, 825-831.
- Rajasekharan, S. and Kennedy, T. E. (2009). The netrin protein family. *Genome Biol.* **10**, 239.
- Sehnert, A. J., Huq, A., Weinstein, B. M., Walker, C., Fishman, M. and Stainier, D. Y. (2002). Cardiac troponin T is essential in sarcomere assembly and cardiac contractility. *Nat. Genet.* **31**, 106-110.
- Suchting, S., Bicknell, R. and Eichmann, A. (2006). Neuronal clues to vascular guidance. *Exp. Cell Res.* **312**, 668-675.
- Suli, A., Mortimer, N., Shepherd, I. and Chien, C. B. (2006). Netrin/DCC signaling controls contralateral dendrites of octavolateralis efferent neurons. *J. Neurosci.* **26**, 13328-13337.
- Tang, X., Jang, S. W., Okada, M., Chan, C. B., Feng, Y., Liu, Y., Luo, S. W., Hong, Y., Rama, N., Xiong, W. C. et al. (2008). Netrin-1 mediates neuronal

- survival through PIKE-L interaction with the dependence receptor UNC5B. *Nat. Cell Biol.* **10**, 698-706.
- Wan, Y., Otsuna, H., Chien, C. B. and Hansen, C.** (2009). An interactive visualization tool for multi-channel confocal microscopy data in neurobiology research. *IEEE Trans. Vis. Comput. Graph.* **15**, 1489-1496.
- Weinstein, B. M.** (2005). Vessels and nerves: marching to the same tune. *Cell* **120**, 299-302.
- Wilson, B. D., Li, M., Park, K. W., Suli, A., Sorensen, L. K., Larrieu-Lahargue, F., Urness, L. D., Suh, W., Asai, J., Kock, G. A. et al.** (2006). Netrins promote developmental and therapeutic angiogenesis. *Science* **313**, 640-644.
- Wolff, C., Roy, S. and Ingham, P. W.** (2003). Multiple muscle cell identities induced by distinct levels and timing of hedgehog activity in the zebrafish embryo. *Curr. Biol.* **13**, 1169-1181.
- Wythe, J. D., Jurynek, M. J., Urness, L. D., Jones, C. A., Sabeh, M. K., Werdich, A. A., Sato, M., Yost, H. J., Grunwald, D. J., Macrae, C. A. et al.** (2011). Hadp1, a newly identified pleckstrin homology domain protein, is required for cardiac contractility in zebrafish. *Dis. Model. Mech.* **4** (in press).
- Yaniv, K., Isogai, S., Castranova, D., Dye, L., Hitomi, J. and Weinstein, B. M.** (2006). Live imaging of lymphatic development in the zebrafish. *Nat. Med.* **12**, 711-716.
- Yebra, M., Montgomery, A. M., Diaferia, G. R., Kaido, T., Silletti, S., Perez, B., Just, M. L., Hildbrand, S., Hurford, R., Florkiewicz, E. et al.** (2003). Recognition of the neural chemoattractant Netrin-1 by integrins alpha6beta4 and alpha3beta1 regulates epithelial cell adhesion and migration. *Dev. Cell* **5**, 695-707.
- Zhou, Q. and Anderson, D. J.** (2002). The bHLH transcription factors OLIG2 and OLIG1 couple neuronal and glial subtype specification. *Cell* **109**, 61-73.